AUTOMATIC HANDLING OF COMMUTATIONS IN BOND GRAPH BASED SIMULATION OF SWITCHED SYSTEMS

Nacusse, Matías A.[a,b] and Junco, Sergio J.[a]

[a] Departamento de Control, Facultad de Ciencias Exactas, Ingeniería y Agrimensura, Universidad Nacional de Rosario, Ríobamba 245 Bis – S2000EKE Rosario – Argentina.
[b] CONICET – Consejo Nacional de Investigaciones Científicas y Técnicas.

[a,b]nacusse@fceia.unr.edu.ar, [a]sjunco@fceia.unr.edu.ar

ABSTRACT
This paper proposes a Bond Graph based solution to the problems of modeling switched physical systems and automatically handling their commutations during the simulation process, featuring the following properties: simultaneous representation of all the operation modes of the switching system in a unique switched Bond Graph, one-to-one correspondence between physical phenomena and model components, and integral-only causality assignment in the Bond Graph storages. To this aim, the Switched Power Junction formalism is used to manage the switching between the different modes, along with a residual-sink-like concept to avoid derivative causality when constraints among energy storages appear, and conservation principles of generalized momentum and charge to re-initialize the state variables when mode switching induces state discontinuities. The proposed solution is illustrated through modeling and simulation of a mechanical and an electromechanical example.

Keywords: Bond Graph, Switched Power Junction, Residual Sinks, Constrained State Variables.

1. INTRODUCTION

Frequently in engineering problems, abrupt changes in physical systems are considered to occur instantaneously. This is mainly so because the phenomena the engineer is interested in have a time scale much bigger than that of the abrupt changes, and that the details inside the time windows of these changes are not relevant to the behavior under study. Thus, ignoring them results in saving modeling time and computational effort. This practice generates a new class of mathematical model, the switched system, where "a logical rule orchestrates switching between a finite number of dynamical subsystems described by differential or difference equations" (Lin and Antsaklis 2007). This paper particularly considers switching among bond graphs (BG) representing different modes of a physical system. This kind of models may arise when modeling under ideal assumptions natural phenomena like mechanical collisions, saturation phenomena, switching in diodes, etc, or technically imposed limitations for safety or commutations for control purposes.

As this practice departs from the assumptions of continuity and smoothness underlying classical physics, it requires special modeling tools as well as suitable simulation and analysis techniques to handle the mathematical models thus obtained, see (Mosterman and Biswas 1998) for a detailed discussion of modeling and simulation issues related to this problem.

Many formalisms for ideal switching modeling have been proposed in the BG domain: MTFs modulated with gain changing between 0 and 1 (Karnopp and Rosenberg 1992), (Asher 1993), (Dauphin-Tanguy and Rombaut 1997); an ideal switch as a new bond graph element (Strömberg, Top, and Söderman 1993); a switch as an ideal current source and a voltage source (Demir and Poyraz 1997); switching bonds (Broenink and Wijbrans 1993); controlled junctions (Mosterman and Biswas 1995, 1998); Petri nets to represent discrete modes and transition between modes (Allard, Helali, Lin, and Morel 1995); and the SPJ or Switched Power Junction formalism. See (Umarikar and Umanand 2005) for an introduction to the latter modeling technique and a brief description and discussion of the pros and cons of all the others. Out of these formalisms, this paper choses the SPJ concept to model mode switching, i.e., the switching among the different BGs, each one of them corresponding to a continuous mode or dynamical subsystem of the switched system. This concept is based on the introduction of two new junction elements, the $\mathbf{0_S}$ or switched-zero junction, and the $\mathbf{1_S}$ or switched-one junction. Using them it is possible to represent all of the switched system operation modes in a unique (switched) BG.

Modeling and simulation of switched systems is particularly defying when nonlinear dynamics is involved and mode changing implies emergence of new and/or disappearance of existing state variables in certain modes, which in the BG domain implies emergence/disappearance of energy storages in integral (and usually also in derivative) causality. Indeed, this latter fact is usually accompanied by discontinuities in the state variables, which calls for re-initialization of state variables immediately after switching. As it is well

known, when such a discontinuity or state jump occurs, there is an instantaneous lost of a finite amount of energy in the system (violation of the energy conservation principle), to which a power impulse is associated. Because of this fact, the values of the state variables after the jump are obtained invoking principles of conservation of generalized momentum or generalized charge, depending upon the kind of energy storages being involved in the state jumps (Borutzky 2004).

In (Junco, Diéguez, and Ramírez 2007) the SPJs have been interpreted in terms of the classical **0**- and **1**-junctions and MTFs modulated by a gain taking the values 0 or 1. In (Nacusse, Junco, and Donaire 2008) the implementation of the $\mathbf{0_S}$ and $\mathbf{1_S}$ as new standard elements of the 20sim basic library has been presented and used in a case study to automatically manage all the mode changes of the switched system without any need of user intervention during the simulation run. From the standpoint of an Object Oriented Modeling (OOM) approach, that work has the drawback of demanding the duplication of the BG components whose causality change due to the mode switching (having more than an object for the same physical phenomenon is a fact that in a certain way collides with the OOM concept). On the other hand, derivative causality unavoidably appears if an I or C component changes causality. Having in mind both aims, to perform the modeling task with an OOM approach, where to each physical phenomenon corresponds a unique BG component, and to avoid derivative causality, the current paper suggests a solution which involves the use of the residual sink concept (Borutzky 2004). This concept is incorporated in 20Sim as the "constraint" sentence (help manual 20Sim 4.1). Its usage is intended to avoid derivative causality in problems like multibody dynamics, where the OOM approach would otherwise force derivative causality when degrees of freedom are lost because the (permanent) coupling of rigid body models. However, if used in switching problems, this sentence assures the satisfaction of the constraints forcing the derivative causality *only* when before commutations there is no discrepancy between the state values to be matched after commutations. In this paper we propose a solution to this problem via the addition of an additional term to the terms usually employed in conjunction with the residual sinks approach. This additional term is just a model of the above mentioned power impulse responsible for the momentum and/or charge conservation during switching. Summarizing, this paper proposes a BG-SPJ based solution to the problem of modeling switched physical systems and automatically handling their commutations during the simulation process, featuring the following properties: simultaneous representation of all the operation modes of the switching system in a unique switched BG, one-to-one correspondence between physical phenomena and BG elements, and integral-only causality assignment in the storages.

Through simple examples Section 2 addresses the background techniques used in the paper: the basics of modeling switched systems using the SPJ method, the principles of momentum and charge conservation during state jumps, and the use of residual sinks to avoid derivative causality in BG. Section 3 recalls the electromechanical application system dealt-with in (Nacusse, Junco, and Donaire 2008). For the sake of comparison, the solution proposed in that paper is first presented, followed by the new solution contributed in this paper. In order to explore the feasibility of the proposed technique to solve complex mechanical problems, Section 4 addresses a mechanical example where somewhat involved calculations are necessary to re-initialize the state variables. Simulation results are provided all along the case studies. Finally, Section 5 presents some conclusions and points out to further work.

2. BACKGROUND RESULTS

The classical continuous BG representations of the continuous modes of a switched system are augmented with the SPJ formalism in order to have a unique and global representation of the whole switched system, which is called a switched bond graph (SwBG). The SPJ-formalism has been selected out of the many ideas and techniques proposed to handle idealized commutations because of its advantages in order to circumvent some associated modeling drawbacks like varying causality of switching-modeling components, hanging junctions, failure to disconnect subsystems, and other inconsistencies (Umarikar and Umanand 2005).

The modeling task is carried out with an OOM approach in which each physical phenomenon has its own and unique BG component. Mode switching could induce causality changes in certain elements, which is not allowed in some M&S software. A way out of this situation is to duplicate the BG component (Nacusse, Junco, and Donaire 2008). This solution works but it does not seem very elegant nor too consistent with the OOM idea. Instead, adding residual sinks to the BG is proposed here in order to prevent from switching causality. An important benefit of this solution is that it allows keeping the preferred integral causality in all the energy storage elements, independently of any causal constraints on their energy variables.

State discontinuity is another phenomenon frequently associated with mode switching. To continue the simulation after such a mode switching, re-initialization of the state variables is necessary. The background computations employed in this paper are based on momentum and charge conservation principles.

All the previous background results are reviewed next.

2.1. Mode switching using SPJ

There are two kinds of SPJ, the $\mathbf{0_S}$ and the $\mathbf{1_S}$, which are **0**- and **1**-junctions admitting more than one bond *graphically* imposing effort or flow on them,

respectively. In the classic BG formalism this presents a causality conflict, because only one bond can impose effort to a **0**- (or flow to a **1**-) junction. However, this causality conflict can be solved adding a constraint via a control variable witch *selects* only one of the imposed efforts (or flows) (Umarikar and Umanand 2005). See appendix A for the basics of SPJs and (Nacusse, Junco, and Donaire 2008) for a generic 20sim implementation of the $\mathbf{0_S}$ and $\mathbf{1_S}$, available for download at http://www.fceia.unr.edu.ar/dsf/I&D/BG.html.

The following example illustrates how to use the SPJ technique. Figure 1 shows a simple electrical circuit which contains two switching elements, an ideal switch (modeling the on-off behavior of a transistor, for instance) and a free-wheel diode. These elements have the complementary logic states {switch open, diode closed} and {switch closed, diode open}. This means that only one control variable is necessary in the SwBG.

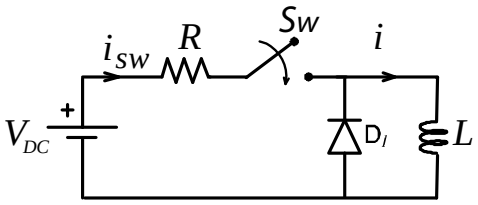

Figure 1: Switched electronic circuit

The current commutations of the ideal switch are modeled with the $\mathbf{1_S}$ and the source $\mathbf{S_f}$ (f≡0), whereas the voltage commutation at the diode is modeled with the $\mathbf{0_S}$ plus the resistor **R** labelled *D1* (it models the diode's conduction state). This yields the SwBG model presented in Figure 2. When the switch is off, the $\mathbf{S_f}$-bond is selected by the $\mathbf{1_S}$ to impose zero current to the submodel to its left, and the $\mathbf{0_S}$ connects the **I** and the **R**(*D1*). When the switch is on, the $\mathbf{1_S}$ disconnects the $\mathbf{S_f}$ and connects the bond on its right side, while the $\mathbf{0_S}$ connects the **I** and disconnects **R**(*D1*).

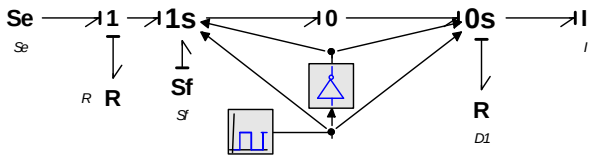

Figure 2: SwBG model

2.2. State variable re-initialization and prevention from derivative causality.

To avoid derivative causality in a BG, a residual sink component is added in order to break the causality constraints (Borutzky 2004). There are two kinds of residual sinks, effort residual sinks *rSe* and flow residual sinks *rSf*. The residual sink injects the necessary effort or flow in order to make vanish the power conjugated variable into the sink. This is *numerically* implemented in 20sim as the *constraint* sentence, but it only works when either the effort or flow is already close to zero.

Here, the need of performing a numerical differentiation is traded against the addition of an algebraic constraint. This constraint is solved off-line in order to also handle the problems associated with state re-initialization when state discontinuities are forced by the system commutations.

The well known electrical example of Figure 3 allows to better see this approach (Borutzky 2004). It shows two electrical RC networks connected by an ideal switch. The ideal switch directly connects two capacitors in parallel.

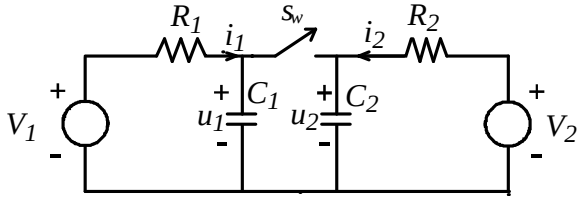

Figure 3: Switched electric circuit

The circuit has two modes of operation, namely mode m_1 and mode m_2, corresponding to open and closed switch, respectively. Switching from m_2 to m_1 does not imply any problem with the initial conditions of the new mode, since there is a smooth transition in the energy variables of the C-elements and the initialization of the new mode is trivial. However, at the instant of a switching from m_1 to m_2, the voltages over the capacitors might be different, so that a state variable re-initialization must be performed. In standard BG modeling two options are available to represent the system in mode m_2: either both C-elements are kept with one of them in derivative causality, or both are combined in a unique equivalent C-element representing the parallel connection. The choice here is the SwBG of Figure 4, a BG where both C-elements are kept in integral causality means the management made by a $\mathbf{1_S}$ junction and an associated switch model featuring a residual sink performing the calculations detailed below in order to inject the current i_S.

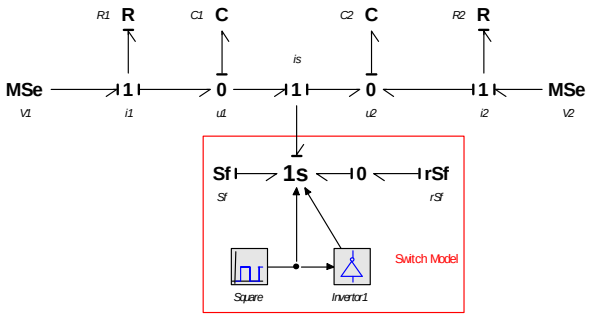

Figure 4: SwBG model.

In mode m_1 the current through the switch is zero and the RC circuits are independent one each other. The SwBG achieves this through the $\mathbf{1_S}$ connecting the flow source with value zero. In mode m_2 the $\mathbf{1_S}$ connects the *rSf* which injects the necessary current to make $u_1=u_2$. This means that the output efforts of both C-elements must be kept equal at all times while the system is in mode m_2. This includes changing instantaneously the (possibly) different efforts in these elements to an equal

and common value when entering this mode. This latter task requires injecting a current impulse, what cannot be done numerically, so that an approximate solution will be provided.

The control law for i_S enforcing the constraint is obtained as follows in terms of the system variables (Borutzky 2004):

$$\begin{aligned} \dot{u_1} &= \frac{1}{C_1}\left(\frac{V_1-u_1}{R_1} - i_s\right) \\ \dot{u_2} &= \frac{1}{C_2}\left(\frac{V_2-u_2}{R_2} + i_s\right) \end{aligned} \quad (1)$$

Calling $i_1 = \frac{V_1-u_1}{R_1}$ and $i_2 = \frac{V_2-u_2}{R_2}$ and defining $u_E = u_1 - u_2$ then:

$$\dot{u_E} = \dot{u_1} - \dot{u_2} = \frac{1}{C_1}(i_1 - i_s) - \frac{1}{C_2}(i_2 + i_s)$$

$$\dot{u_E} = \frac{1}{C_1}i_1 - \frac{1}{C_2}i_2 - \frac{C_1+C_2}{C_1C_2}i_s \quad (2)$$

So, if:

$$i_s = \frac{C_1C_2}{C_1+C_2}\left(\frac{1}{C_1}i_1 - \frac{1}{C_2}i_2\right) \quad (3)$$

Then

$$\dot{u_E} = 0$$

Equation (3) enforces the constraint $u_1 \equiv u_2$ only if the two voltages are equal at t_C^+, the time instant immediately after commutation. If this condition does not hold –which is the normal situation after a switching from m_1 to m_2–, then a constant error between u_1 and u_2 appears. A remedy to this problem is to add an extra term in equation (3), as shown in (4).

$$i_s = \frac{C_1C_2}{C_1+C_2}\left[\frac{1}{C_1}i_1 - \frac{1}{C_2}i_2 + K_E u_E\right] \quad (4)$$

If K_E is chosen to be the Dirac impulse applied at the commutation instant, i.e., $K_E = \delta(t - t_C)$, then the additional term becomes

$$\frac{C_1C_2}{C_1+C_2}\delta(t - t_C)u_E(t_C^-)$$

which is exactly the impulsive current producing the charge transfer from one capacitor to the other which instantaneously equalizes their voltages, see (Borutzky 2004) for instance. Of course, in a numerical simulation the Dirac impulse can be only approximatively implemented as a square pulse, for instance, of high value and correspondingly short time-base.

Another option would be to let K_E be a high-value constant defining the speed of asymptotic convergence between u_1 and u_2, as the resulting error dynamics $\dot{u_E} = -K_E u_E$ shows. Even if it works, it is easily seen that in the BG domain this amounts to connect a **R**-element with very low resistance value (high admittance K_E), which implies a stiff system when the SwBG is in mode m_2. This is not desirable, as one of the reasons for the choice of the SPJ approach was to avoid alternatives like inserting parasitic elements, precisely because the stiffness induced by them.

An third alternative, exactly equivalent to have the Dirac impulse in the extra term in (4), is provided by 20sim. It involves resetting the integrators associated to each storage whose energy variable jumps. To this aim, the regular integration sentence *int(x, init)* must be replaced by *resint(x,newoutp,reset,init)*, see (Nacusse, Junco, and Donaire 2008) for an application example and also the 20sim manual for more details.

Figure 5 show the results of a simulation implemented in 20sim of the SwBG depicted in Figure 4. The flow residual sink *rSf* is implemented by a modulated flow source with equation (4) as control law, with the impulse approximately realized as a pulse, as above discussed. The simulation scenario is as follows, the switch is commanded by a square signal with period *T=10 s* starting in m_2. The voltages source V_1 is a sine wave with amplitude 100 volts and V_2 is a constant voltage source of 120 volts. The parameters of the circuit are: *R1=2MΩ, C1=0.1μF, R2=1MΩ, C2=1μF* and K_E has amplitude equal to K_E*=1000* during 1ms

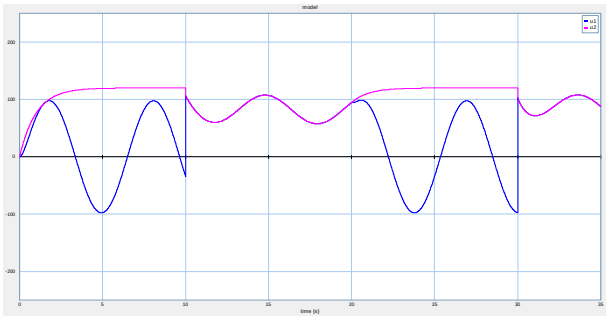

Figure 5: Capacitors voltages u_1 (blue) and u_2 (magenta)

3. APLICATION EXAMPLE: SERIES DC MOTOR WITH SWITCHED CIRCUIT FOR FIELD WEAKENING.

Figure 6 shows the application example presented in this section in order to illustrate the approach explained in the previous sections. The example consists of a series DC motor with switched circuit for field weakening (Leonhard 1997). Equations 5 are the electromechanical conversion relationships, where *K* is a constructive constant and *g(.)* is the nonlinear magnetic characteristic of the excitation field.

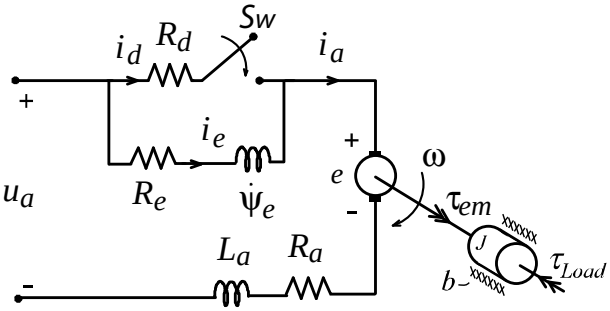

Figure 6: Equivalent circuit of series DC motor.

$$\begin{aligned} \tau_{em} &= K\Psi_e i_a \\ e &= K\Psi_e \omega \\ \Psi_e &= g(i_e) \end{aligned} \tag{5}$$

In this configuration the motor operates in two modes: in the full field (FF) mode when the switch is open and in field weakening (FW) mode when the switch is closed. The FF mode is used when the motor speed is below the base (nominal) speed and the FW mode is used for higher motor speeds.

3.1. Full excitation mode.

Figure 7 shows the BG model in the FF operation mode. In this figure the nonlinear I element representing the excitation winding is in derivative causality. As explained in section 2.2, to avoid derivative causality a residual sink element is properly placed in the BG, see Figure 8.

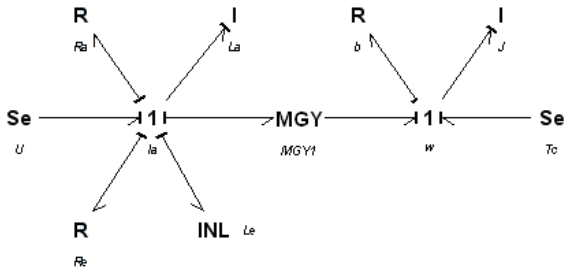

Figure 7: FF BG with derivative causality

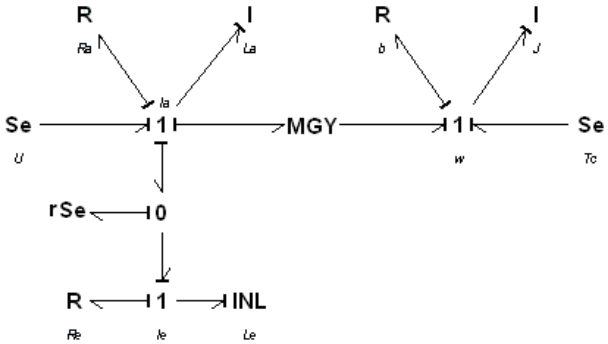

Figure 8: FF BG with all elements in integral causality

3.2. Field weakening mode.

Figure 9 shows the BG model in the FF operation mode. The corresponding state equations are given in (6).

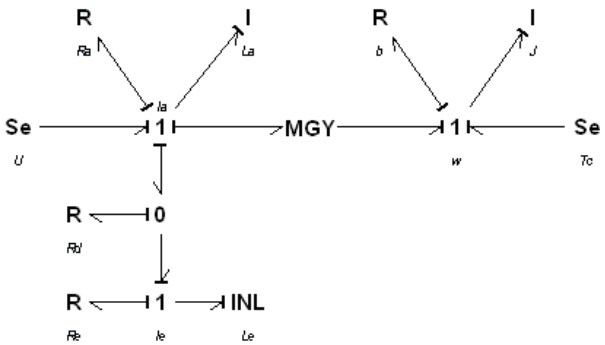

Figure 9: FW BG model

$$\begin{aligned} \dot{\imath_a} &= -\frac{K}{L_a}\Psi_e\omega - \frac{(R_a+R_d)i_a}{L_a} - \frac{R_d}{L_a}g^{-1}(\Psi_e) + \frac{U}{L_a} \\ \dot{\Psi_e} &= R_d i_a - (R_e + R_d)g^{-1}(\Psi_e) \\ \dot{\omega} &= -\frac{b}{J}\omega + \frac{K}{J}\Psi_e i_a - \frac{\tau_c}{J} \end{aligned} \tag{6}$$

Entering in the FW mode does not present any problem because there is no jump in the energy variables. On the contrary, when the system passes from FW mode to FF mode discontinuities appear in the energy variables associated to both electrical I-elements, so that the initial conditions for the simulation of the FF mode must be calculated.

3.3. Switched BG models of Series DC-Motor

Combining the BG of Figures 7 and 9 the SwBG model of Figure 10 is obtained, which has been previously presented in (Junco, Diéguez, and Ramírez 2007). The excitation winding has been duplicated to handle the causality switching caused by the commutation.

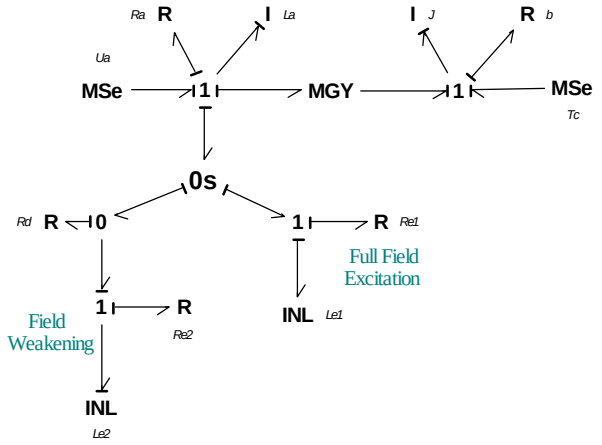

Figure 10: SwBG with derivative causality and duplicated elements: **1**, **INL** (Le1,2) and **R** (Re1,2).

The only differences between Figures 8 and 9 are the residual sink element (FF mode) and the R component labelled *Rd* (FW mode), which represents the field weakening resistance R_d. Both components impose effort to the zero junction. This means that a $\mathbf{0_s}$ SPJ can be used to connect either the residual sink or the field weakening resistor, as shown in the SwBG model of the series DC-motor of Figure 11. Equations 7 show the state equations read from this SwBG. The auxiliary variable U_S impressed by the $\mathbf{0_S}$ has been used.

$$\begin{aligned} \dot{\imath_a} &= \frac{U}{L_a} - \frac{R_a}{L_a}i_a - \frac{K}{L_a}\Psi_e\omega - \frac{U_S}{L_a} \\ \dot{\Psi_e} &= U_s - R_e g^{-1}(\Psi_e) \\ \dot{\omega} &= \frac{K}{J}\Psi_e i_a - \frac{b}{J}\omega - \frac{\tau_c}{J} \end{aligned} \tag{7}$$

When the DC motor is in FW mode, then $U_s = R_d(i_a - i_e)$ and equations 7 coincide with equations 6. For FF operation U_s is calculated as follows:

Be $U_1 = U - R_a i_a - K\Psi_e\omega$ and $U_2 = R_e g^{-1}(\Psi_e)$

Then, rewriting the first two equations of 7 in term of i_a and i_e:

$$\dot{i_a} = \frac{U_1 - U_s}{L_a}$$
$$\dot{i_e} = \frac{U_s - U_2}{g'(i_e)} \qquad (8)$$

Where $g'(i_e) = \frac{\partial g}{\partial i_e}$ .Then, defining $\dot{i_\delta} = \dot{i_a} - \dot{i_e}$ and performing the same steps as in section 2.2 yields:

$$U_s = \frac{L_a g'(i_e)}{L_a + g'(i_e)} \left[\frac{1}{L_a} U_1 + \frac{1}{g'(i_e)} U_2 + K_E i_E \right] \qquad (9)$$

Mutatis mutandis, K_E plays here for the current error the same role as in (4) for the voltage error.

$$\dot{i_E} = -K_E i_E \qquad (10)$$

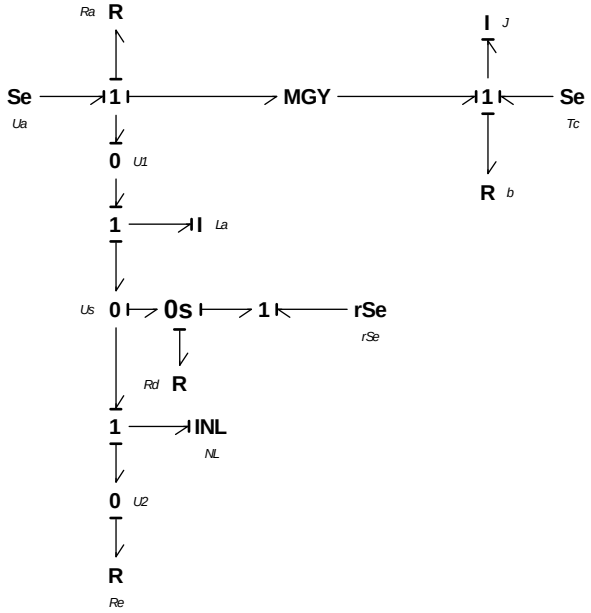

Figure 11: SwBG. All storages in integral causality.

3.4. Simulations Results

To make the simulations more realistic a cascade control system is added, where a PI-speed controller runs a hysteresis-band current controller, see (Leonhard 1997) for details. The block diagram of the cascade control system is shown in Figure 12. Figure 13 shows the internal block diagram of the switch control block, which connects/disconnects the field weakening resistor. The logic signal Switch is one for FF mode and is zero for FW mode. Figure 14 shows the 20sim implementation of overall control scheme. The block called Series DC-Motor contains the SwBG model of Figure 11. The effort residual sink *rSe* is implemented by a modulated effort source with equation 9 as control law. The motor parameters used in the simulation are: U_a=*1000 V*; base speed ω_B = *1910 rpm*, R_a=*9.89 mΩ*, L_a=*1.4 mH*, R_e=*14,85 mΩ*, R_d=*16,96 mΩ*, *K=0.04329 Nm/WbA*, *J=3 Kgm2*, T_{Load}=*1370 Nm.*

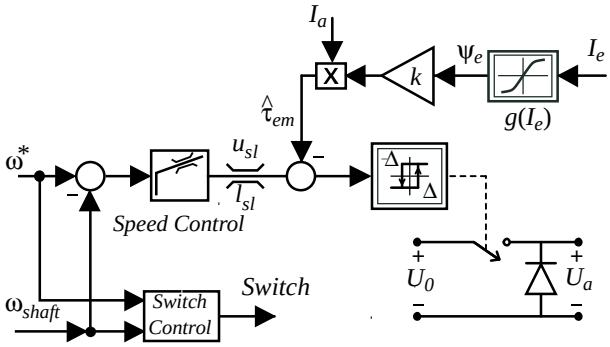

Figure 12: Block diagram SwBG model

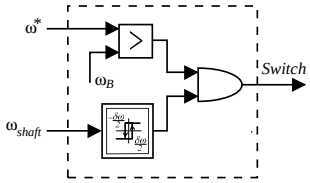

Figure 13: Switch Control Block

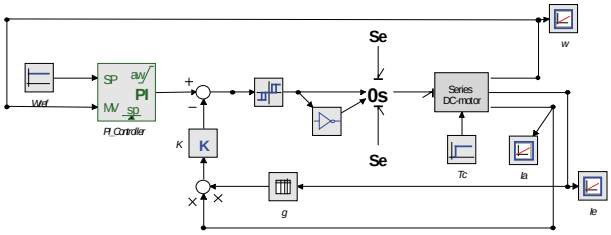

Figure 14: 20sim implementation of the control scheme.

Figure 15 shows the speed profile followed by the motor. The motor speed decrement at time *T=3sec* is produced by the load torque application. Figure 16 shows the armature current i_a, the excitation current i_e and the switch state.

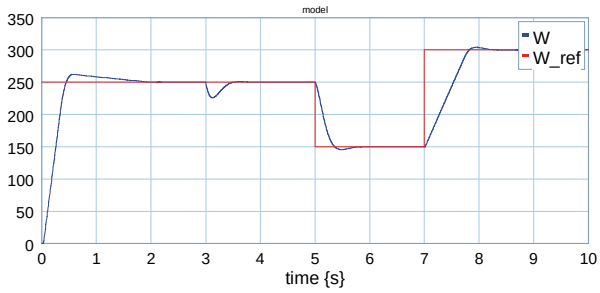

Figure 15: Reference (red) and motor speed (blue).

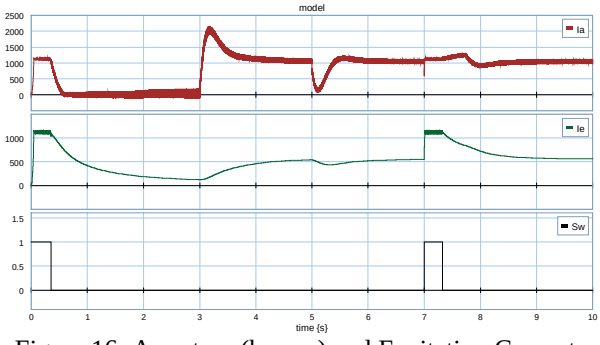

Figure 16: Armature (brown) and Excitation Current (green). Switch state (black).

4. MECHANICAL EXAMPLE:

Figure 17 shows an idealized physical system of a slider crank mechanism. The slider crank mechanism transforms rotational into translational motion, or vice-versa.

The rotation wheel is attached to the mass by means of a rigid and massless bar with longitude *l*. This implies that one of the *I* elements in the BG must be in derivative causality.

Avoiding derivative causality can be performed in different ways. Here, it is achieved splitting in two the MTF-element linking the rotational and translational inertias, as shown in the SwBG of Figure 18. Friction has been modeled associated to both motion coordinates (linear models with coefficients b_1 and b_2).

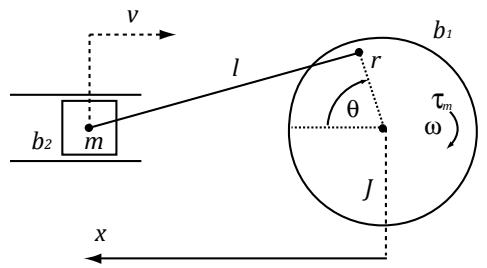

Figure 17: Idealized Physical System of a Slider crank mechanism.

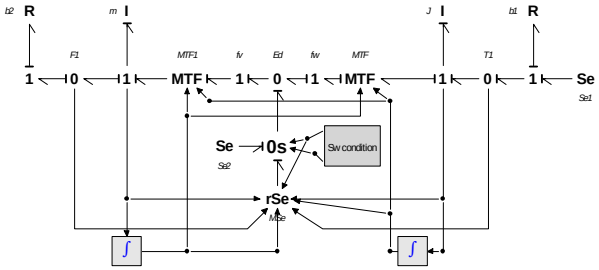

Figure 18: SwBG model of the Slider crank mechanism.

The MTF-elements have the following gains:

$$f_v = \frac{(x - r\cos\theta)}{l} v \qquad (11)$$

$$f_\omega = \frac{(rx\sin\theta)}{l} \omega \qquad (12)$$

Where equation 11 corresponds to the *MTF1* element and equation 12 to *MTF* depicted in Figure 18.

In order to obtain the control law for the residual sink we can write the state equations of the system as:

$$\dot{v} = \frac{1}{m}\left[\frac{(x - r\cos\theta)}{l} E_D - F_1\right]$$

$$\dot{\omega} = \frac{1}{J}\left[\tau_1 - \frac{rx\sin\theta}{l} E_D\right]$$

Where F_1 is the fiction effort in the mass *m*, $\tau_1$is the input torque minus the friction torque and E_D is the effort injected by the residual sink. Defining $f_E = f_w - f_v$ as the flow error, the control law for the residual sink can be obtained performing the same steps as in the previous examples.

$$E_D = \left[\frac{(x - r\cos\theta)^2}{ml^2} + \frac{(rx\sin\theta)^2}{Jl^2}\right]^{-1} \left[\frac{(rx\sin\theta)}{Jl}\tau_1 + \frac{(x - r\cos\theta)}{ml} F_1 + \frac{v^2 + xr\omega^2\cos\theta - 2v\omega r\sin\theta}{l} + K_E f_E\right]$$

The parameters used in the simulation were: $J=0.124Nm^2$, $b_1=0.1Kgm/s$, $r=0.5m$, $l=2$, $m=8Kg$, $b_2=15.Kg/s$ (Rideout and Stein 2003).The simulation starts with the mass at rest in position $x=1.6m$ and disconnected from the wheel. An input torque of constant value $\tau_{in}=250Nm$ is applied to the wheel at time $T=0s$. At time $T=2.368s$ the wheel is connected to the mass. The angle θ at connection time is $\theta=1.192rad$ (68.3degrees).

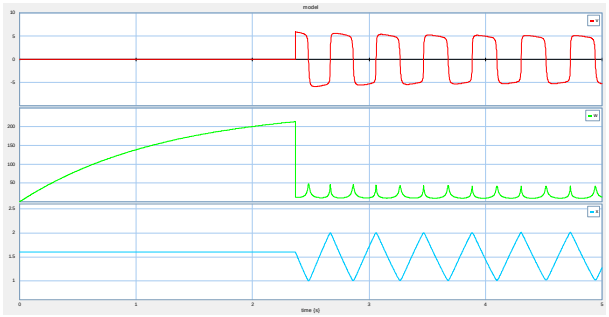

Figure 19: Response of the slider crank mechanism. Mass speed (red) and position (light blue), angular speed (green).

A correct response is observed in the simulation figures, particularly the discontinuities in both the translational and the angular speeds at the collision-like coupling time can be appreciated.

This example has been included in order to test the applicability of the proposed methodology to mechanical problems where the constraints among energy variables often involves nonlinear functions of the state variables, i.e., through much more complex relationships as in the first two examples. This is the case, for instance, when the multibody modeling and simulation approach is employed for mechanical systems subject to collision-like connection of 3D-bodies composing the overall system.

5. CONCLUSIONS.

The problem of modeling and simulation of physical systems undergoing switching and state discontinuities has been addressed in the bond graph domain. A solution has been proposed to automatically handling the commutations during the simulation process, featuring the following properties: simultaneous representation of all the operation modes of the switching system in a unique switched Bond Graph, one-to-one correspondence between physical phenomena and model components, and integral-only causality assignment in the Bond Graph storages. The Switched Power Junction formalism has been used to represent the switching between the different modes, while the residual-sink was the resource employed to avoid derivative causality when constraints among

energy storages appear, and conservation principles of generalized momentum and charge have been resorted to in order to re-initialize the state variables when mode switching induces state discontinuities. The proposed solution has been demonstrated through modeling and simulation of a mechanical and an electromechanical example. Further work aims at applying the method to complex mechanical systems undergoing collision and constrained coupling modeled with the multibody dynamics approach.

ACKNOWLEDGMENTS

The authors wish to thank CONICET (the Argentine National Council for Scientific and Technological Research) and SeCyT-UNR (the Secretary for Science and Technology of the National University of Rosario) for their financial support.

APPENDIX A: SWICHED POWER JUNCTIONS

Figure 20 show the SPJ with causality assignment.

Only one of the control variables is allowed to have the value 1 at a given time instant, the rest are zero.

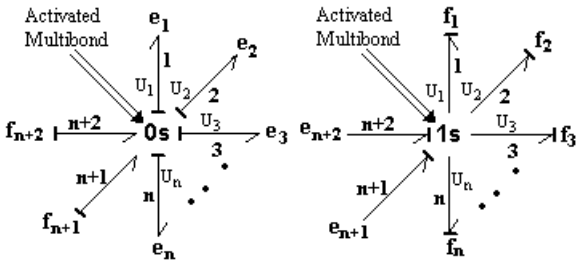

Figure 20: Switch Power Junctions with causality assignment.

Equations 13 and 14 express the mathematical relationship, for the $\mathbf{0_S}$ and the $\mathbf{1_S}$ respectively, between the power variables and the control signals injected to select the appropriate bond.

$$\begin{aligned} &\text{Effort} = U_1 e_1 + U_2 e_2 + \cdots + U_n e_n \\ &f_i = U_i (f_{n+1} + f_{n+2}) \quad ; \; i = 1, \ldots, n \end{aligned} \tag{13}$$

$$\begin{aligned} &\text{Flow} = U_1 f_1 + U_2 f_2 + \cdots + U_n f_n \\ &e_i = U_i (e_{n+1} + e_{n+2}) \quad ; \; i = 1, \ldots, n \end{aligned} \tag{14}$$

APPENDIX B: RESIDUAL SINKS

The residual sink component injects the necessary effort or flow in order to make vanish the power conjugated variable into the sink.

A residual sink element can be interpreted as an energy store where it parameter tend to zero. For example, an effort residual sink can be interpreted a C element in integral causality:

$$C\dot{e} = \Delta f$$

If the parameter C tends to zero, then $\dot{e}$ is determined by the algebraic equation $\Delta f = 0$.

Figure 21 shows the graphical representation of the effort and flow residual sink used in (Borutzky 2009).

Figure 21: Effort and flow residual sink

REFERENCES

Allard, B., Helali, H., Lin, Ch., Morel, H., 1995. Power converter average model computation using the bond graph and Petri Net Techniques. *IEEE Power Electronic Specialist Conference*, pp. 830–836.

Asher, G., 1993. The robust modeling of variable topology circuits using bond graphs. *Proc. Int. Conf. on Bond Graph Modeling and Simulation*. San Diego, CA, pp. 126–131.

Borutzky, W., 2004. *Bond Graphs. A Methodology for Modelling Multidisciplinary Dynamic Systems*. Erlangen, San Diego: SCS Publishing House.

Borutzky, W., 2009. Bond graph model-based fault detection using residual sinks. *Proc. IMechE, Part I: Journal of Systems and Control Engineering*, Vol. 223, pp. 337-352, London: PEP.

Broenink, J. and Wijbrans, K., 1993. Describing discontinuities in bond graphs. *Proceedings of International Conference on Bond Graph Modelling*. San Diego, CA, pp. 120–125.

Controllab Products B.V., 20-sim™, http://www.20sim.com/

Dauphin-Tanguy, G. and Rombaut, C., 1997. A Bond Graph Approach For Modeling Switching Losses of Power Semiconductor Devices. *Proc. Int. Conf. on Bond Graph Modeling and Simulation*. pp. 207-212.

Demir, Y. and Poyraz, M., 1997. Derivation of state and output equations for systems containing switches and a novel definition of switch using the bond graph model. *Journal of the Franklin Institute*. 3343 (2) 191–197.

Lin, H. and Antsaklis, P., 2007. Switching Stabilizability for Continuous-Time Uncertain Switched Linear Systems. *IEEE Transactions on automatic control*. Vol. 52, N°4, April 2007. pp 633-646.

Help 20sim 4.1 Controllab Products B.V., 20-sim™, http://www.20sim.com/webhelp.html

Junco, S., Diéguez, G., Ramírez, F., 2007. On commutation modeling in Bond Graphs, *Proc. Int. Conf. on Bond Graph Modeling and Simulation*, San Diego, CA, pp. 12-19.

Karnopp, D. and Rosenberg, R., 1992. *System Dynamics. A Unified Approach*, 2nd ed., Wiley Interscience, New York.

Karnopp, D., Margolis, D., Rosenberg, R., 2000. *System Dynamics. Modeling and simulation of mechatronic systems*, 3rd edition, Wiley Interscience, New York.

Leonhard, W., 1997. *Control of Electrical Drives*. New York. Springer-Verlag.

Mosterman, P. and Biswas, G., 1995. Behaviour generation using model switching. A hybrid bond graph modeling technique. *Proc. Int. Conf. on Bond Graph Modeling and Simulation*, Las Vegas, pp. 177–182.

Mosterman, P. and Biswas, G., 1998. A theory of discontinuities in physical systems models. *Journal of the Franklin Institute*, 335B (3), 401–439.

Mosterman, P., 1997. *Hybrid Dynamic Systems. A hybrid bond graph modeling paradigm and its application in diagnosis*. Ph.D. Thesis, Vanderbilt University, Nashville, Tennessee, USA.

Nacusse, M., Junco, S., Donaire, A., 2008. Automatizando el Modelado y Simulación con Bond Graph de sistemas Físicos Conmutados. *Mecánica Computacional.* XXVII, pp. 3479-3494.

Rideout, G. and Stein, J., 2003. An Energy-Based Approach to Parameterizing Parasitic Elements for Eliminating Derivative Causality. *Proc. Int. Conference on Bond Graph Modeling and Simulation*, Orlando, FL.

Strömberg, J., Top, J., Söderman, U., 1993. Variable causality in bond graph caused by discrete effects. *Proc. Int. Conf. on Bond Graph Modeling and Simulation*, San Diego, CA, pp. 115–119.

Umarikar, A. and Umanand, L., 2005. Modelling of switching systems in bond graphs using the concept of switched power junctions. *Journal of the Franklin Institute*, Vol. 342, pp. 131-147.